Journal of
Marine Science and Engineering

MDPI

Article

Numerical Research on a T-Foil Control Method for Trimarans Based on Phase Lag

Yifang Sun [1,2], Yiqun Wang [1], Dapeng Zhang [1,*], Zongduo Wu [1] and Guoqing Jin [3]

[1] Ship and Maritime College, Guangdong Ocean University, Zhanjiang 524088, China; 4u@stu.gdou.edu.cn
[2] Guangdong Provincial Engineering Research Center for Ship Intelligence and Safety, Zhanjiang 524000, China
[3] Liaoning Engineering Laboratory for Deep-Sea Floating Structures, School of Naval Architecture, Dalian University of Technology, Dalian 116024, China
* Correspondence: zhangdapeng@gdou.edu.cn

Abstract: The lift force of a T-foil, which varies with ship motion, can counteract the wave exciting force during wave encounters. The phase difference between the periodic lift force and the wave exciting force significantly impacts the T-foil's effectiveness. This study investigates the phase difference between lift force and motion to optimize the control equation for the T-foil's angle, thereby reducing negative feedback. The T-foil's hydrodynamic performance is first calculated using computational fluid dynamics. Time-domain calculations of the phase lag between lift force and motion under open-loop control in still water are then used to determine the dimensionless phase lag of the T-foil's angle at various frequencies, facilitating further optimization of the control method. Finally, calculations of trimaran heave and pitch in regular waves are conducted. The results demonstrate that, under phase lag control, the T-foil's lift force phase precedes ship motion by approximately 0.2 s, reducing hysteresis in the anti-vertical motion effect. Comparisons of vertical hull motions between different control methods reveal a 20% reduction in vertical motion with phase lag control compared to pitch control. This study concludes that phase lag is a crucial factor in T-foil control optimization.

Keywords: T-foil; vertical motion; phase lag; torque control

Citation: Sun, Y.; Wang, Y.; Zhang, D.; Wu, Z.; Jin, G. Numerical Research on a T-Foil Control Method for Trimarans Based on Phase Lag. *J. Mar. Sci. Eng.* **2024**, *12*, 1209. https://doi.org/10.3390/jmse12071209

Academic Editor: Rodolfo T. Gonçalves

Received: 17 May 2024
Revised: 11 July 2024
Accepted: 15 July 2024
Published: 18 July 2024

1. Introduction

Trimarans consist of two side bodies and a main body. All three pieces are slender, and the main body's aspect ratio is between 12 and 18, which helps to reduce wave-forming resistance when sailing at high speeds. Therefore, trimarans have an advantage over traditional ships in terms of speed and resistance [1]. However, trimarans are likely to create noticeable heave and pitch motions when sailing at a high speed or in a high sea state, which increases the rate of seasickness, decreases speed, and increases the slamming load. A T-foil installed on the bow can neutralize wave disturbances by producing a vertical force and moment in the opposite direction to the ship's motion when sailing. This can then be used to suppress the ship's vertical motion. The T-foil control system has been upgraded recently with the automatic control program. This allows the system to alter the attack angle in real time in response to the ship's motion and to modify the force's direction and amount in real time, producing a more noticeable effect [2,3].

The control of the T-foil requires two elements, the prediction of the force relationship during the ship's motion and the design of the control method. Regarding the former, research on trimaran hydrodynamic performance has been greatly aided by the development of CFD (computational fluid dynamics) technology in recent years. Studies in this area have demonstrated the method's ability to accurately calculate the trimaran's motion and force in the time domain [4–6]. When it comes to the control method, the conventional practice is to build a force–motion transfer function to reduce motion through PID (Proportional Integral Differential) control. This is done by linearizing the ship's motion under

the influence of waves and introducing the lift model of anti-vertical motion equipment (T-foil) [7–10]. An essential part of designing active control systems is determining the transfer function between force motion and rectifying the control parameters; accurate hydrodynamic performance estimates must be used to determine the control parameters.

T-foil and stern flapped foils have been installed on a high-speed monohull ship by DL Cruz and Giron-Sierra et al. since 2000 [11,12]. They have utilized the computational fluid dynamics (CFD) method to determine the hydrodynamic force coefficient of bare ship models under various sea states and speeds, and on this basis to establish the transfer function between waves, force, and motion. After that, they introduced the lift force (moment) model of the T-foil and eventually designed a multi-objective optimized PID control procedure for the rate of seasickness, the cavitation phenomenon, and mechanical efficiency. The motion response of the ship following the implementation of active T-foil control was calculated using dynamic system simulation in this program. The findings indicated that the high-speed ship's vertical acceleration was lowered by 65%, and the incidence of seasickness was reduced by 35% [13].

Alavimehr investigated the open-loop control of the navigation state control system in still water based on the passive control of the T-foil [14,15]. In this method, the T-foil's horizontal sheet continuously rotates in response to sinusoidal signals to measure the motion of the ship model brought on by the lift force (moment). The final test results provided the basis for additional navigation state control system refinement. They identified the combination of the swing angles of the T-foil and the stern flaps when the model was allowed to produce only heave (while the pitch angle of the model was close to 0°) or pitch (while the heave displacement of the model was close to 0 mm) motion.

Jiang and Bai have introduced a non-linear control method for the T-foil, called step control [16,17]. The T-foil's horizontal foil deflected in response to either the pitch angular velocity or the local velocity signal at the T-foil installation site. The T-foil's angle deflected to the opposite maximum angle if the direction of velocity changed. Next, a hybrid control strategy that incorporates step and linear controls has been put forth. To ensure that the maximum angle of the T-foil conforms to the CI (control intensity) multiplied by signal amplitudes, a parameter known as CI is introduced for the approach. Finally, the heave, pitch, and local acceleration of the Wigley model III are predicted under four control strategies at two forward speeds (Froud Number, Fr = 0.3, 0.5). The findings demonstrate that the hybrid control significantly reduces the vertical motions while providing the benefits of both linear and step controls.

Liu [18] designed a stabilization controller for motion reduction of trimarans. The dimensions and installation position of the T-foil and flap, which were chosen as the stability appendages, were supplied. The control strategy relied on the notion of the moment and force as a result of using the Kalman filter. Finally, the experimental results demonstrate the effectiveness of the appendages and the proposed controller.

The effect of the T-foil can be greatly enhanced by controlling its lift force (moment) by the use of the ship's motion signals, such as the heave velocity, pitch angular velocity, or pitch angle. Nonetheless, previous studies have demonstrated that the ship's inertia results in a phase difference between the external force and the motion of the ship, and the phase lag effect generates a short delay between the effective force and its effect. The phase difference between the lift force and the ship's motion will increase negative feedback to the T-foil control, which will ultimately decrease the T-foil's effect. To effectively mitigate the impact of wave disturbances, the T-foil's actual control should be placed slightly ahead of the ship's motion. However, most previous investigations have directly controlled the rotation of the T-foil according to the existing motion signals and have rarely considered the phase lag effect.

In practical applications, the vertical motion of a ship is readily measurable, yet the phase of the wave exciting force slightly precedes this motion. Since the time-varying lift force should correlate with the wave exciting force, it is essential to investigate the phase difference between force and motion. This understanding can then be used to optimize

T-foil control methods based on phase lag. By adjusting control parameters accordingly, active T-foils can more effectively suppress vertical motion.

In this study, a trimaran has been considered as the primary objective of this article. At first, the ship's motion and the lift of the T-foil were modeled using CFD technology. The relationship between the lift force and the attack angle was fitted using the static airfoil theory. The trimaran's motion in waves was confirmed to be reliable using the overlapping grid technology, and the ship's pitch and heave hydrodynamic force coefficients were computed using forced oscillations. The ship's motion was then calculated in the time domain, the phase difference under each frequency was summarized using the time-record curve, the control equation was optimized, and the control parameters were computed. Next, the open-loop control of the T-foil was calculated in still water, and the T-foil's angle was controlled in real time with different frequencies. Last, using dynamic modeling technology, the trimaran's motion at two speeds in regular waves was numerically simulated. The ship's responses under the static T-foil, pitch angle signal control, and phase lag control were then compared to verify the T-foil's effect.

2. Modeling of the Ship's Motion Controlled by T-Foil

The modeling and hydrodynamic performance calculation of the ship and its appendages are the foundation for the motion and control problem of the trimaran, allowing the active control method of the T-foil to be suggested and optimized. The trimaran's motion in regular waves is calculated by optimizing the mathematical model of the lift force (moment) of the T-foil by determining the relationship between the lift force and the attack angle of the T-foil.

2.1. Mathematical Modeling of the Ship's Motion and T-Foil

Ships, as partially submerged objects, possess six degrees of freedom in their motion: heave, sway, surge, pitch, roll, and yaw. Three coordinate systems are employed: the geodetic coordinate system $O_1x_1y_1z_1$, the reference coordinate system $O'x'y'z'$, and the moving coordinate system $Oxyz$, as shown in Figure 1.

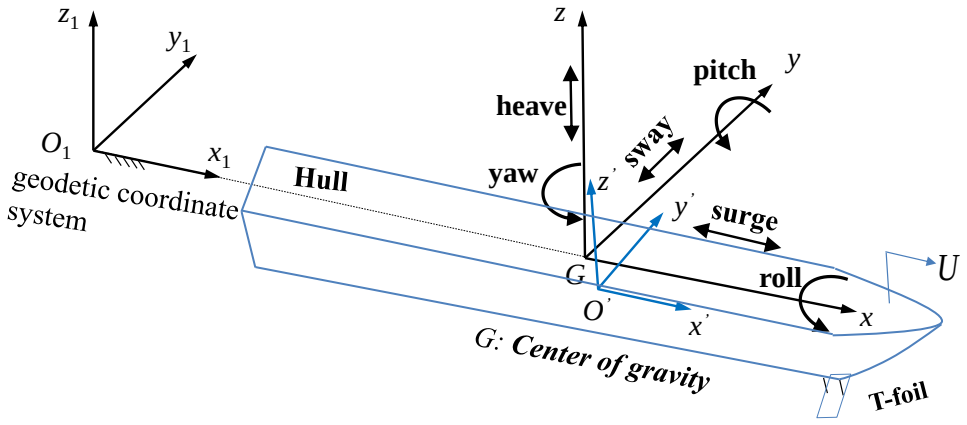

Figure 1. Coordinate systems.

When a ship sails against waves, it encounters regular waves with small amplitudes. These waves generate radiation fluid force and wave disturbance force, leading to small amplitude motion. Assuming the ship is divided symmetrically by the X-Z vertical plane, the six differential equations can be decoupled into two sets, as shown in Figure 2. Equation (1) can then be used to derive the ship's longitudinal motion equation when the T-foil generates vertical control force f_T and moment M_T. Given the focus on longitudinal motions and their attenuation, the heave and pitch motions are of primary interest in this research.

$$\begin{aligned}(m + a_{33})\ddot{z} + b_{33}\dot{z} + c_{33}z + a_{35}\ddot{\theta} + b_{35}\dot{\theta} + c_{35}\theta = F_3 - f_T\\ (I_y + a_{55})\ddot{\theta} + b_{35}\dot{\theta} + c_{55}\theta + a_{53}\ddot{z} + b_{53}\dot{z} + c_{53}z = M_5 - M_T\end{aligned} \quad (1)$$

where z is the heave displacement, θ is the pitch angle, m is the ship's mass, and I_y is the moment of inertia of pitching. a_{ij} represents the additional mass of the motion in the i, or j, direction or the moment of inertia of the additional mass (i, j = 3,5), b_{ij} represents the damping force (moment) coefficient of the motion in i, j direction (i, j = 3, 5), c_{ij} represents the restoring force (moment) coefficient of the motion in the j, i direction (i, j = 3, 5), F_3 is the vertical force of the wave against the ship, M_5 is the pitch moment of the wave against the ship.

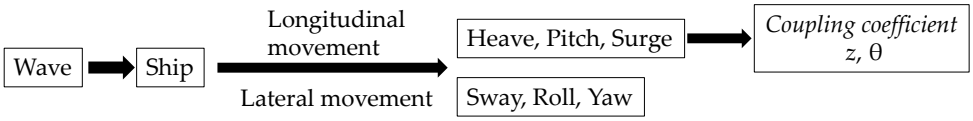

Figure 2. Functional block diagram for the derivation of motion equation.

The horizontal foil's swing angle, or the angle of deflection of the T-foil's horizontal foil to the middle position, is related to the attack angle (α) of the T-foil. It is also influenced by the ship's pitch angle (θ), pitch angular velocity ($\dot{\theta}$), heave velocity ($\dot{z}$), and the distance between the T-foil's installation position and the ship's longitudinal center of gravity (LCG) l_F [19]. Based on the static lift theory, and with the memory effect of the flow field ignored, the lift force (moment) F_T and moment M_T are expressed by the lift coefficient C_L, as shown in Equation (2):

$$\begin{cases} f_T = \frac{1}{2}\rho U^2 A \frac{dC_L}{d\alpha}\alpha \\ M_T = \frac{1}{2} l_F \rho U^2 A \frac{dC_L}{d\alpha}\alpha \end{cases} \quad (2)$$

where l_F is the distance between the installation position of the T-foil and the longitudinal center of gravity (LCG) of the ship. By substituting Equation (2) into Equation (1), the motion equation of the ship under the action of the T-foil can be obtained as Equation (3):

$$\begin{cases} (m + a_{33})\ddot{z} + b_{33}\dot{z} + c_{33}z + a_{35}\ddot{\theta} + b_{35}\dot{\theta} + c_{35}\theta = F_3 - \frac{1}{2}\rho U^2 A \frac{dC_L}{d\alpha}(\varphi + \theta - \frac{l_F\dot{\theta}+\dot{z}}{U}) \\ (I_y + a_{55})\ddot{\theta} + b_{35}\dot{\theta} + c_{55}\theta + a_{53}\ddot{z} + b_{53}\dot{z} + c_{53}z = M_5 - \frac{1}{2} l_F \rho U^2 A \frac{dC_L}{d\alpha}(\varphi + \theta - \frac{l_F\dot{\theta}+\dot{z}}{U}) \end{cases} \quad (3)$$

2.2. Calculation of Hydrodynamic Performance of T-Foil

Based on Equation (2), the lift force f_T and lifting moment M_T of a T-foil at various attack angles are determined by its lift coefficient derivative $dC_L/d\alpha$, once parameters such as profile, foil span, and chord length are established. The computational fluid dynamics program STAR CCM+ (Version 11.04) facilitates the calculation of the relationship between lift coefficient C_L and attack angle α, enabling an analysis of hydrodynamic properties.

Figure 3 shows the mesh partition, with the T-foil profile being NACA0012. The main scale parameters and basic mesh dimension parameters are provided in Tables 1 and 2. The T-foil's swing angle is restricted to $\pm 10^\circ$ to prevent stalling during movement. Figure 2 illustrates the meshing of the T-foil model.

The T-foil is fully submerged in water in this calculation, the incoming flow velocity is 2.115 m/s, and the turbulence model used is k-ω turbulence. Eleven working conditions with the attack angle of the oncoming flow as 0°, $\pm 10^\circ$, $\pm 8^\circ$, $\pm 6^\circ$, $\pm 4^\circ$, and $\pm 2^\circ$ are selected. The lift values generated by the T-foil are calculated with a time step of 0.001 s, and the calculation time is cut off until the force is stabilized. The T-foil's lift coefficients are linearly fitted to the change in attack angle. The results are displayed in Figure 4 and are deemed to be a good fit by computing the coefficient of determination R^2. This shows that $dC_L/d\alpha$ *is* 3.3483.

Figure 3. Meshing of the T-foil model.

Table 1. Dimensions of T-foil.

Index	Value
Airfoil shape	NACA0012
Wingspan/mm	240
Chord length/mm	100
Aspect ratio	2.667
Max angle/(°)	±10
Max angular velocity/(Hz)	2.4
Length of vertical foil/mm	60

Table 2. Basic mesh dimension parameters.

Index	Value
Volume of computational domain/m	0.6 × 0.18 × 0.48
Maximum size of mesh/m	0.0025
Minimum size of mesh/m	0.000625
Layers of boundary layer mesh	13
Growth rate of boundary layer	1.5
1st layer thickness of boundary layer/mm	0.02
Total quantity of grid	988 thousand

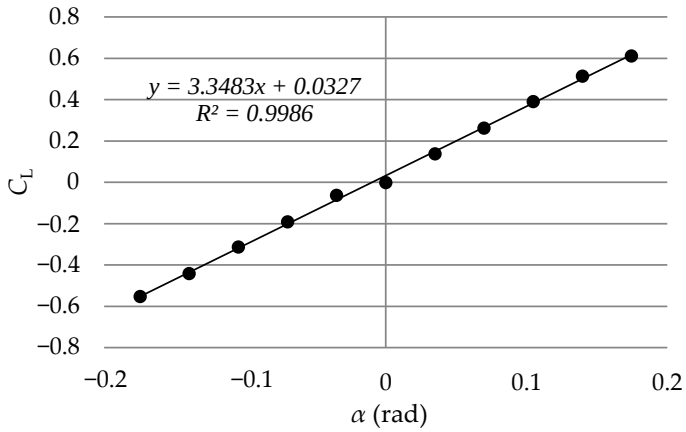

Figure 4. Lift coefficient dependence on the attack angle.

2.3. Calculation of the Kinematic Response of Trimaran

2.3.1. Mesh Partition

To ensure the accuracy of the estimated findings, STAR CCM+ is used to compute the trimaran's motion response in a regular wave when the T-foil (fixed swing angle) is acting on it. The *k*-ε turbulence model is chosen because it is suitable for solving complex geometric external flow problems. The first-order volume-of-fluid (VOF) method and the deep-water approximation strategy are adopted to produce regular waves and capture free liquid surfaces. The only parameters that need to be stated are the wave direction, wavelength, and height. The two degrees of freedom of the motion of the ship's heave and pitch are solved by DFBI (Deliberate Foreign Body Ingestion).

The boundary conditions consist of five velocity inlets and one pressure outlet (Figure 5). The computational domain is divided into two sections using overlapping grid technology: the background basin and the overlapping grid region. VOF wave damping is applied within 2 m of the pressure outlet to suppress waves. The trimaran's shape parameters align with previous research [20], with the portion above the waterline raised sufficiently to prevent deck wetness. The underwater profile, displacement, moment of inertia, and center of gravity position remain unchanged to ensure the hydrodynamic performance of the numerical model is consistent with that of the test model. The total number of ship meshes is 5.46 million, with mesh partitioning illustrated in Figure 6. Table 3 presents the ship's main dimensions.

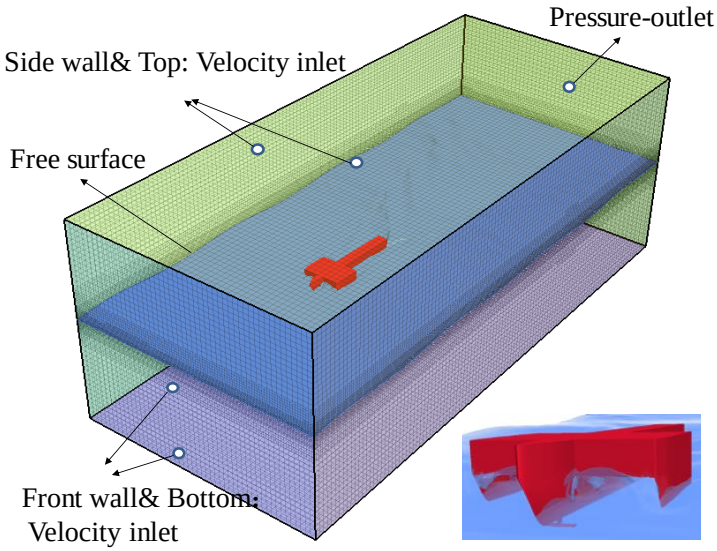

Figure 5. Boundary condition setting.

Table 3. Main particulars of the physical model.

	Main Hull	Side Hulls
Length overall/m	4.0	1.0
Breadth of waterline/m	0.3584	0.085
Draught/m	0.17	0.10
Displacement/kg	129.07	4.45
Wetted surface/m^2	1.899	0.201
Block coefficient	0.530	0.524

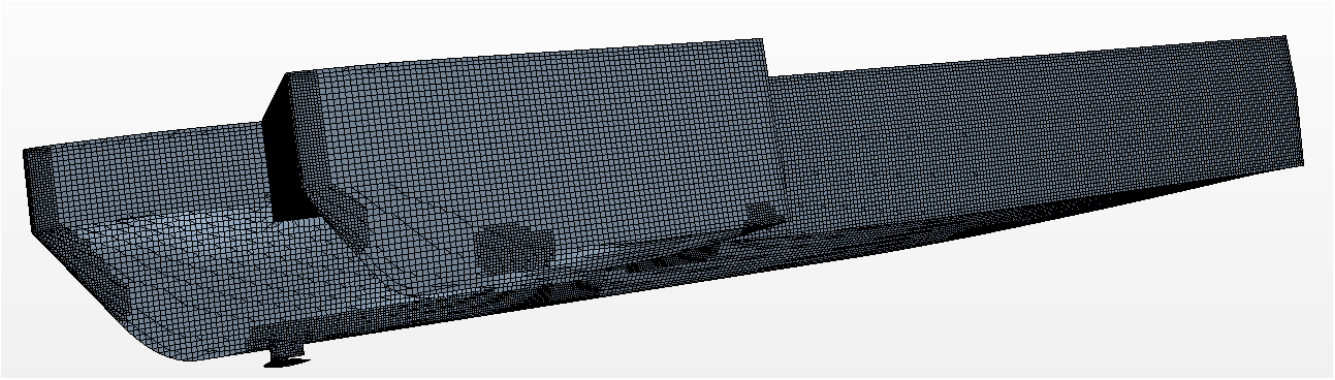

Figure 6. Surface mesh of the trimaran model.

2.3.2. Verification of Reliability of Calculations

The mathematical model of the proposed control system was derived and validated against experimental results obtained from model tests conducted in the Towing Tank at Dalian University of Technology. This ITTC member facility features a tank 170 m long, 7 m wide, and 3 m deep, equipped with side wall wave dampers and a 20-flap wavemaker. A 1:25 scale model of a trimaran with a transom stern was used, with side hull dimensions obtained by shrinking the main hull by a factor of four. The model was attached to a seaworthiness instrument installed on the carriage. The model's main particulars correspond to those of the numerical model shown in Table 1.

To validate the independence of the time step, the F_r = 0.338 is chosen, which corresponds to a speed of 2.115 m/s, wave height of 0.046 m, and wavelength of 10 m. The time-record curves of pitch and heave for the model with various time steps (e.g., 0.01 s, 0.005 s, and 0.0025 s) were computed and compared with the experimental findings, as illustrated in Figure 7a,b. The computations at two time steps of 0.005 s and 0.0025 s are highly similar to one another, and the deviations of pitch and heave calculated by both of them are within 5%. The computations also demonstrate that the fluid's flow distance at a single time step is not greater than one mesh, which satisfies the convergence condition.

Furthermore, if the computation correctness is guaranteed, choosing the right mesh number size might increase calculation efficiency. The models with a time step of 0.005 s were chosen under identical working conditions, and the three mesh models' time-record curves for heave and pitch were compared, as illustrated in Figure 7c,d. The time-record curves of the three mesh models are nearly identical, with a deviation of less than 5%, so the 5.46 million mesh model is selected for subsequent computation.

To confirm the accuracy of the ship's motion calculation under the influence of the T-foil, the model is further moved against the waves in a regular wave with a wave height of 0.046 m and a wavelength of 4~10 m at a speed of 2.115 m/s after the mesh number and time step are established. A comparison between the calculated results of heave and pitch motion of the model equipped with a fixed T-foil in regular waves and the results of the model test is shown in Figure 8. The horizontal coordinate is the encounter frequency ω_e; the vertical coordinate is the dimensionless heave value (2 z/H) in Figure 8 and the pitch angle in Figure 9. The figures show that there is less than 20% relative error between the numerical prediction and the model test results.

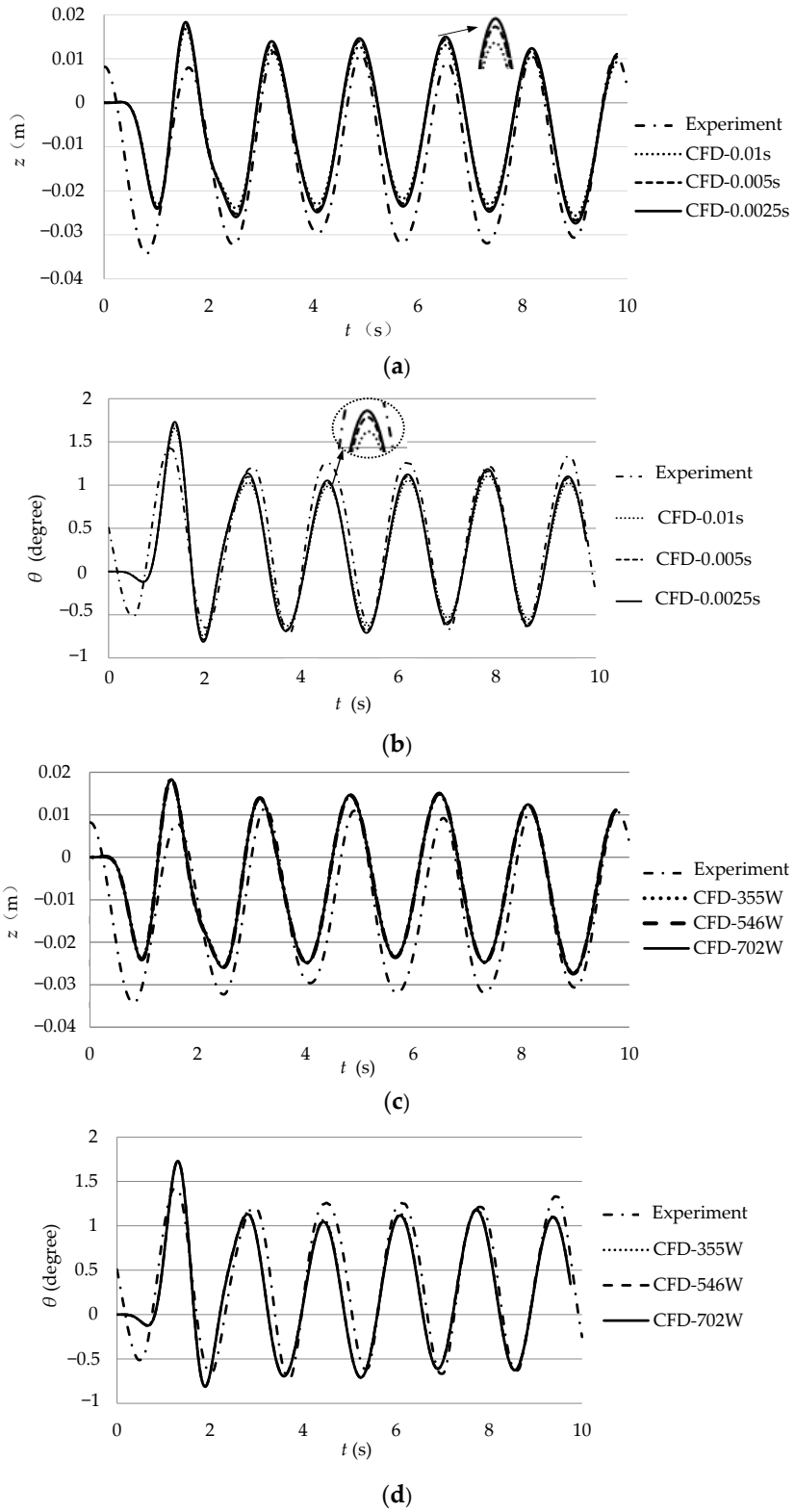

Figure 7. Convergence verification of calculation. (**a**) Time-record curves of heave with different time steps (λ = 10 m, U = 2.115 m/s). (**b**) Time-record curves of pitch with different time steps (λ = 10 m, U = 2.115 m/s). (**c**) Time-record curves of heave with different grid quantities (λ = 10 m, U = 2.115 m/s). (**d**) Time-record curves of pitch with different grid quantities (λ = 10 m, U = 2.115 m/s).

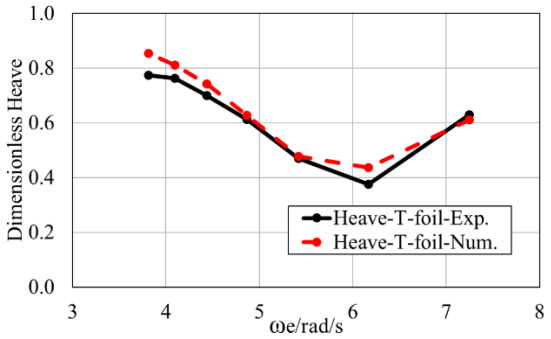

Figure 8. Dimensionless heave for trimaran with T-foil.

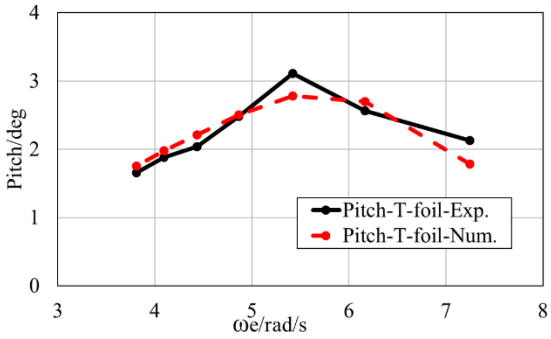

Figure 9. Pitch angle for trimaran with T-foil.

3. Open-Loop Control in Still Water

The T-foil reduces the ship's vertical motion by generating vertical forces and moments that neutralize wave disturbance forces. The ship's velocity has a phase lag about the vertical force because of its inertia, and the lag period varies with the encounter frequency. The time-domain examination of the phase relationship between the lift force of the T-foil and the motion of the ship is used to integrate the control variables and parameters, analyze the phase difference between the two, and optimize the control equations.

3.1. Open-Loop Control of T-Foil

In still water, the wave exciting force is negligible, simplifying Equation (1)–(4):

$$\begin{aligned}(m + a_{33})\ddot{z} + b_{33}\dot{z} + c_{33}z + a_{35}\ddot{\theta} + b_{35}\dot{\theta} + c_{35}\theta = f_T \\ (I_y + a_{55})\ddot{\theta} + b_{35}\dot{\theta} + c_{55}\theta + a_{53}\ddot{z} + b_{53}\dot{z} + c_{53}z = M_T\end{aligned} \quad (4)$$

Ship motion is generated by the T-foil's lift force (and moment) when the attack angle varies over time. The ship will produce regular heave and pitch motions by entering a sinusoidal signal with a predetermined frequency into the field function tool of STAR CCM+ and allowing the T-foil's swing angle to oscillate with the period to form a periodic pendent force (moment). The control signal of the swing angle φ of the T-foil is given by Equation (5):

$$\varphi = \varphi_0 \cos \omega' t \quad (5)$$

where $\varphi_0 = 10^\circ$ and is the maximum value of the T-foil's swing angle, and ω' is the swing angle frequency, matching the encounter frequency of the ship in regular waves. As mentioned in the preceding section, the mesh number for the ship and T-foil is 5.46 million, and the computing time step is 0.0025 s. Table 4 outlines the computational conditions. To study the effect of speed on T-foil performance, two typical sailing speeds are selected: U = 2.115 m/s (Fr = 0.3, hull-borne speed) and U = 3.2 m/s (Fr = 0.5, semi-planning speed). This allows for the calculation of changes in ship heave amplitude and pitch angle over time.

Table 4. Conditions of calculation in open-loop control.

	ω' (rad/s)							
Fr = 0.3	8.95	7.29	6.16	5.41	4.87	4.44	4.09	3.80
Fr = 0.5	11.27	9.04	7.54	6.56	5.87	5.3	4.86	4.49

Figures 10 and 11 depict the time-record curves of lift force under fixed-frequency T-foil angle swings for two conditions (Fr = 0.3, ω' = 6.16 rad/s; Fr = 0.5, ω' = 7.54 rad/s). The lift force can reach more than 25 N in Fr = 0.3, and as the speed increases, it can reach 70 N in Fr = 0.5. Figures 10 and 11 illustrate the T-foil's effect on the ship, with time on the abscissa, heave displacement z and pitch angle θ on the primary ordinate, and T-foil swing angle φ on the secondary ordinate. The T-foil's lift force (and moment) produces a pitch angle of approximately 1.5° and a heave amplitude of 18 mm at low speed. At high speed, these values increase to 2° and 30 mm, respectively. The heave frequency aligns with the T-foil swing frequency, albeit with a minor phase lag of 0.23 s (roughly 0.2 cycles). Pitch motion, with an amplitude of approximately 1.2°, mirrors the heave and coincides with the T-foil swing frequency. The pitch phase slightly leads the heave phase, lagging behind the swing angle by approximately 0.17 s.

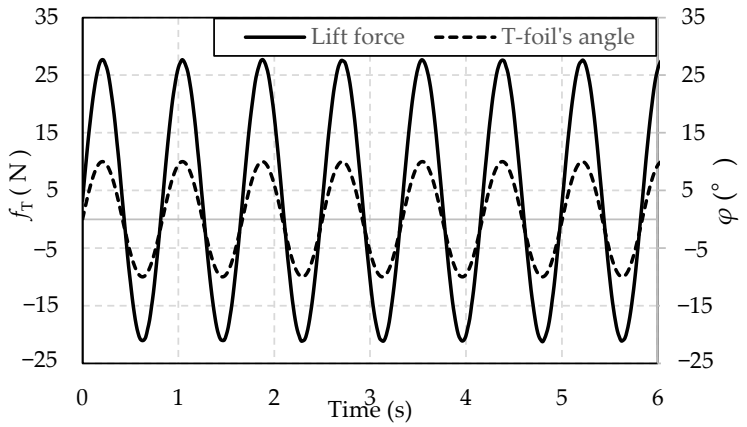

Figure 10. Time-record curves of lift force (Fr = 0.3).

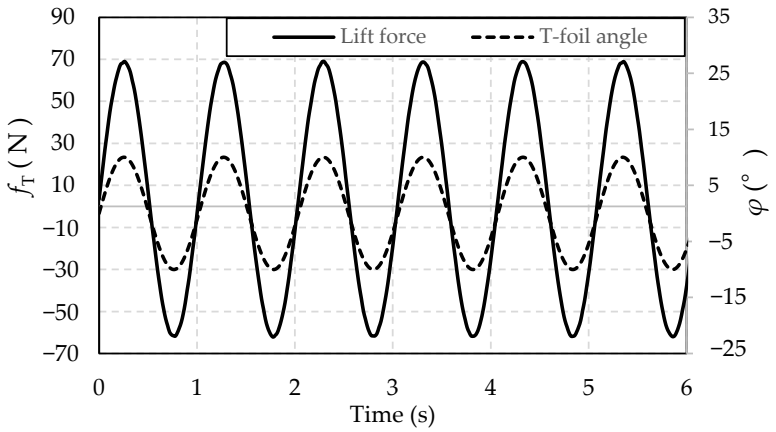

Figure 11. Time-record curves of lift force (Fr = 0.5).

The time-record curves of the model's pitch and heave at a high speed (Fr = 0.5) as a result of the T-foil's action are displayed in Figure 12a–d, respectively. The heave amplitude, which fluctuates periodically with the lift force and has a lag time of 0.23 s (0.3 cycles), is around 18 mm, which is significantly less than the motion at a higher speed. As the speed

increases, the influence of the T-foil becomes more noticeable. The pitch amplitude is about 2°, with a lag time of 0.26 s, slightly lower than the heave motion. This shows that the increase in lift torque reduces the phase lag of the pitch.

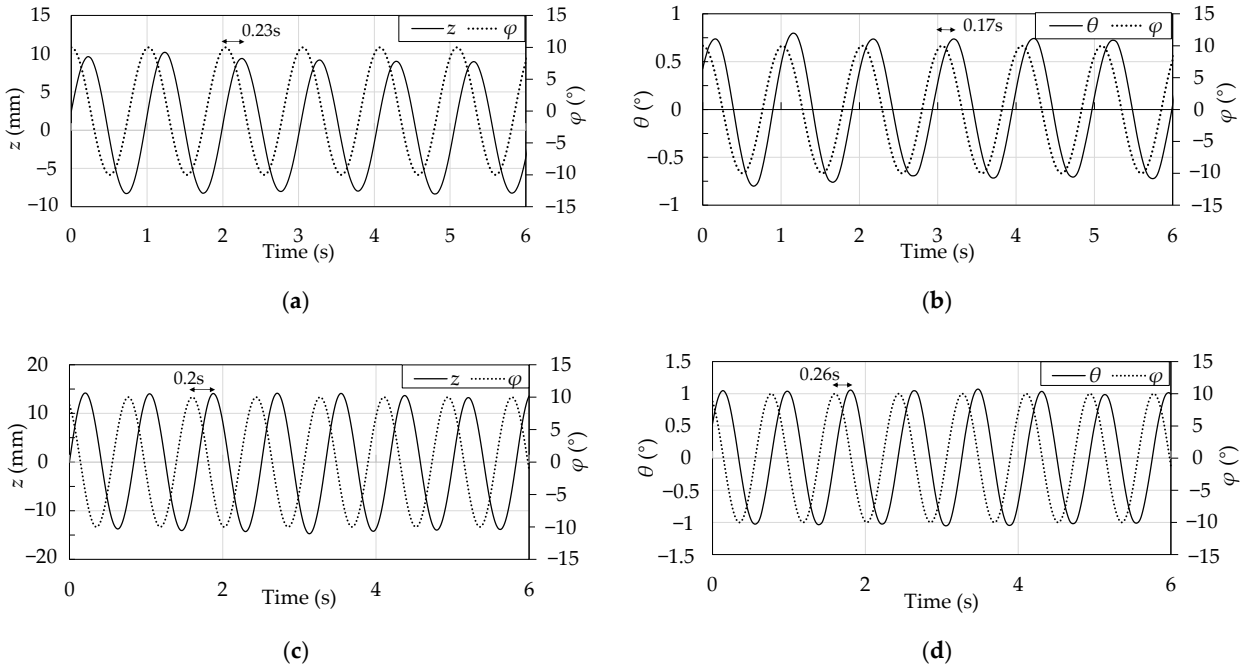

Figure 12. Time-record curves of swing angle and motions. (**a**) Heave amplitude and swing angle (Fr = 0.3). (**b**) Pitch angle and swing angle (Fr = 0.3). (**c**) Heave amplitude and swing angle (Fr = 0.5). (**d**) Pitch angle and swing angle (Fr = 0.5).

The phase difference of the heave and pitch motion of the horizontal foil of the T-foil at each oscillation frequency is shown in Tables 5 and 6, respectively. As shown in Figures 13 and 14, the data are dimensionless, allowing the determination of the phase lag's number of cycles. T' is a non-dimensional period given by

$$T' = \frac{\Delta T}{T} \tag{6}$$

where ΔT is the time of phase lag between the T-foil's angle and the ship's motion, and T is the ship's period of motion.

Table 5. Phase lag of heave and pitch (Fr = 0.3).

ω'	Heave Lag (s)	Pitch Lag (s)
11.233	0.311	0.352
8.950	0.273	0.295
7.531	0.202	0.253
6.555	0.171	0.204
5.838	0.153	0.194
5.288	0.102	0.145
4.850	0.043	0.098
4.492	0.011	0.021

Table 6. Phase lag of heave and pitch (*Fr* = 0.5).

ω'	Heave Lag (s)	Pitch Lag (s)
8.960	0.261	0.301
7.246	0.238	0.279
6.167	0.211	0.261
5.418	0.161	0.224
4.864	0.142	0.201
4.435	0.095	0.158
4.092	0.031	0.096
3.810	0.012	0.054

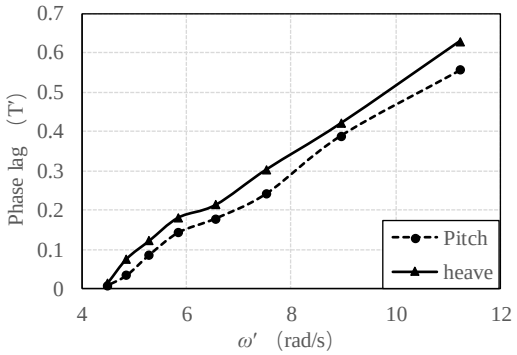

Figure 13. Dimensionless phase lag (*Fr* = 0.3).

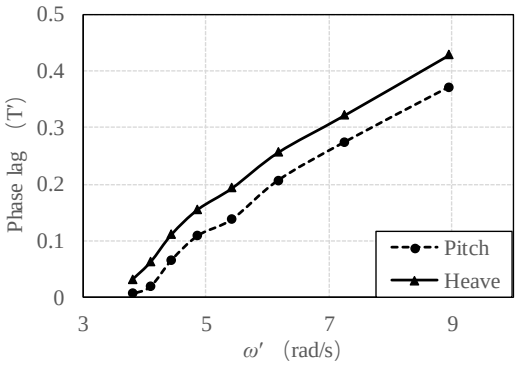

Figure 14. Dimensionless phase lag (*Fr* = 0.5).

When traveling at low speeds and high frequencies, the phase lag time of the pitch and heave is greater than 0.2 s or roughly 0.3–0.6 cycles, and it diminishes as the T-foil oscillation frequency reduces. At low frequencies, the phase lag issue is not as significant. This is because the force effect is mostly unaffected by inertia at lower swing frequencies, where the rate of change in lift force with time is smaller. The trends of the heave and pitch motions are similar, with the phase of the pitch ahead of that of the heave at high frequencies by about 0.05 s. When the trimaran sails at a low speed, the phase lag issue at high speeds is slightly smaller as the lift increases, but the trends remain similar. The uncaused phase lag at high frequencies is between 0.2 T' and 0.6 T'. In general, the T-foil oscillation frequency of the ship at two speeds in regular waves is consistent with the values found in Tables 5 and 6. Consequently, the phase lag between the vertical motion and lift force can exceed 0.3 encounter periods in the high responsiveness zone of the ship's motion ($\lambda \in [4,6]$, $\omega_e \in (5,9)$). Due to the negative feedback caused by the hysteresis effect of the lift, the T-foil's control method needs to take into account the effect of the phase difference.

3.2. T-Foil's Control Method

When the ship is swaying significantly, the active T-foil can achieve the goal of anti-vertical motion by altering the attack angle in real time and subsequently producing a larger reverse lift (moment). According to previous studies [21], the rotation of the horizontal foil of the T-foil is controlled in real time by using the lifting moment control, i.e., the lifting moment M_T generated by the T-foil is in the opposite direction of the motion of the ship (including heave and pitch motions), and C_i is the control parameter; then, the lifting moment can be obtained by Equation (7):

$$M_T = -C_1\theta' - C_2\dot{\theta} - C_3\ddot{\theta} \tag{7}$$

When the profile of the T-foil is selected, if its attack angle $|\alpha| \leq \alpha_1$ and α_1 is the stall angle of the foil, then at a certain constant water speed, $\frac{1}{2}\rho U^2 A \frac{dC_L}{d\alpha}$ is a constant and is set to K_F. By combining Equations (3) and (7), we obtain Equation (8):

$$\varphi = -\frac{C_3}{K_F l_F}\ddot{\theta} + (1 - \frac{C_1}{K_F l_F})\theta - (\frac{C_2}{K_F l_F} + \frac{l_F}{U})\dot{\theta} + \frac{1}{U}\dot{z} + \frac{C_1}{K_F l_F}\theta_0 \tag{8}$$

where θ_0 is the stern inclination angle, which can be calculated numerically or through testing with $\theta' = \theta - \theta_0$ and is influenced by the speed U. The installation position, the horizontal foil's lift performance, the ship's velocity, and other factors all affect the T-foil's swing angle. Determining the control parameter C_i is crucial to figuring out the control equation.

To reduce the negative feedback effects of the hysteresis effect, as mentioned in Section 2.1, the lift force of the T-foil at certain encounter frequencies should be ahead of the pitch or lifting–sinking motion by a specific amount of time. Therefore, due to the different phases of θ, $\dot{\theta}$, and $\ddot{\theta}$, the values of C_1, C_2, and C_3 need to be reasonably adjusted to meet the phase difference of lift force and motion. The "trial and error method" can be used to find control parameters. For example, pitch control measures the lift force (moment) of the T-foil against the ship's pitch angle. The value of C_1 can be initially calculated based on the movement of the ship under the fixed foil, as the maximum swing angle of the T-foil $\pm\varphi_0$ and the pitch angle of the highest value of θ_{max} are known:

$$C_1' = \frac{\varphi_0}{\theta_{max} - \theta_0} K_F l_F \tag{9}$$

where $C_1{}'$ is the pre-adjusted value of C_1. After taking into account the impact of phase lag time, C_2 and C_3 are added and adjusted further to modify the phase φ until it satisfies the computational needs for the pitch angle lag time of 2.1 and guarantees that it is near, but not more than, φ_0. Since the ship sails in regular waves, the value of C_i is kept constant with time at each encounter frequency. Similar steps can be taken to regulate the heave motion. By modifying C_1, C_2, and C_3 by the heave lag time, an additional set of C_i can be obtained. The result of this computation can be employed as the control parameter in the force–motion transfer function equation in the dynamic simulation. The values of C_i under the control of the hysteresis effect are displayed in Tables 7 and 8.

Table 7. Values of C_i (i = 1, 2, 3) in heave phase lag control.

Fr	C_i	λ = 3 m	λ = 4 m	λ = 5 m	λ = 6 m	λ = 7 m	λ = 8 m	λ = 9 m	λ = 10 m
0.3	C_1	65.05	75.621	180.564	295.32	320.21	305.32	315.215	301.487
	C_2	5.214	6.325	10.213	20.654	25.321	28.365	30.547	35.698
	C_3	11.953	10.365	15.154	14.521	12.354	15.852	13.325	12.587
0.5	C_1	223.215	172.245	203.2	186.325	350.3	360.32	267.32	245.32
	C_2	20.365	15.32	18.356	14.325	20.357	40.254	65.322	56.478
	C_3	21.256	23.42	32.874	28.248	21.732	30.589	32.6	20.336

Table 8. Values of C_i (i = 1, 2, 3) in pitch phase lag control.

Fr	C_i	λ = 3 m	λ = 4 m	λ = 5 m	λ = 6 m	λ = 7 m	λ = 8 m	λ = 9 m	λ = 10 m
0.3	C_1	60.254	72.325	156.892	270.124	305.956	312.980	405.980	285.632
	C_2	8.215	10.352	12.520	30.696	30.658	30.548	35.784	40.698
	C_3	9.235	9.001	10.385	8.673	7.589	3.698	4.589	7.365
0.5	C_1	174.200	163.580	175.630	152.963	330.250	320.210	248.365	200.050
	C_2	24.897	18.021	24.156	26.965	21.368	32.169	70.365	62.002
	C_3	19.919	14.916	21.629	12.021	4.216	2.886	4.021	5.926

4. Calculation of Active Control

4.1. Principles of Numerical Simulation

The longitudinal motion of the trimaran, after being subjected to wave action while sailing against waves, can be expressed by Equation (4), where the right side of the equation is the algebraic sum of the wave disturbance force (moment) and the lift force (moment) of the T-foil, denoted as F_3' and M_5'. The ship is subjected to wave forces, which produce longitudinally coupled motions, including heave and pitch motions. The workflow of the simulation system is displayed in Figure 15, with $G(s)$ serving as the "force–motion" transfer function and s as the independent variable. The linear acceleration and angular acceleration produced by the ship are integrated to obtain the velocity and displacement. The motion signals are then processed by the T-foil controller, and the real-time swing angle of the T-foil can be obtained by the control equations. This generates the lifting force (moments) against the wave disturbing force and accomplishes the purpose of controlling the motion.

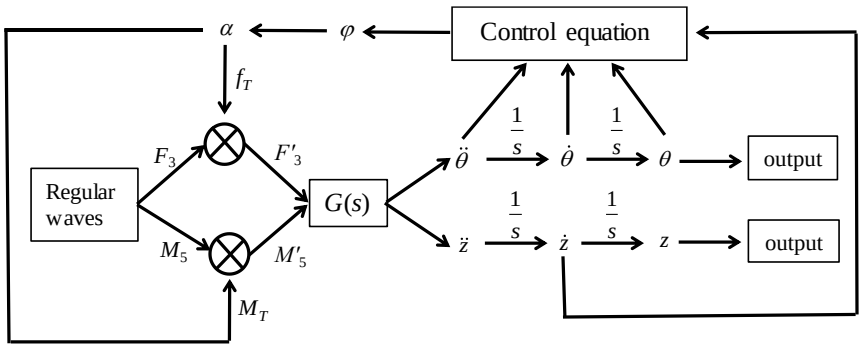

Figure 15. Flow chart of trimaran's vertical motion control system.

The pitch, lifting, and sinking motions of the ship are a set of coupled motions, reflected in the coupling of the transfer function $G(s)$. Equation (3) is solved in the frequency domain by the Laplace transform (with zero initial condition):

$$\begin{cases} \left[(m+a_{33})s^2+b_{33}s+c_{33}\right]Z(s)+\left(a_{35}s^2+b_{35}s+c_{35}\right)Q(s)=F_3'(s) \\ \left[\left(I_y+a_{55}\right)s^2+b_{55}s+c_{55}\right]Q(s)+\left(a_{53}s^2+b_{53}s+c_{53}\right)Z(s)=M_5'(s) \end{cases} \tag{10}$$

where $Z(s)$ and $Q(s)$ are the transfer functions of the heave displacement and pitch angle, respectively. Equation (10) can be written in matrix form as

$$\begin{bmatrix} (m+a_{33})s^2+b_{33}s+c_{33} & a_{35}s^2+b_{35}s+c_{35} \\ a_{53}s^2+b_{53}s+c_{53} & \left(I_y+a_{55}\right)s^2+b_{55}s+c_{55} \end{bmatrix}\begin{bmatrix} Z(s) \\ Q(s) \end{bmatrix}=\begin{bmatrix} F_3'(s) \\ M_5'(s) \end{bmatrix} \tag{11}$$

Thus, solving for

$$\begin{bmatrix} Z(s) \\ Q(s) \end{bmatrix}=\begin{bmatrix} (m+a_{33})s^2+b_{33}s+c_{33} & a_{35}s^2+b_{35}s+c_{35} \\ a_{53}s^2+b_{53}s+c_{53} & \left(I_y+a_{55}\right)s^2+b_{55}s+c_{55} \end{bmatrix}^{-1}\begin{bmatrix} F_3'(s) \\ M_5'(s) \end{bmatrix}=G(s)s^2\begin{bmatrix} F_3'(s) \\ M_5'(s) \end{bmatrix} \tag{12}$$

it is evident that the external forces and moments F_3' and M_5', which determine the lift force (moments) and the corresponding hydrodynamic coefficients a_{ij}, b_{ij}, and c_{ij}, are necessary to obtain numerical computations of the ship's motion to determine either of the output outputs (heave amplitude or pitch angle).

4.2. Simulation and Control Design

The entire system is made up of four modules, as illustrated in Figures 16–19, which are the modules for wave force input, force motion, swing angle calculation, and lift force (moment) calculation of the T-foil. The dynamic simulation and numerical modeling are based on the Simulink module of Matlab R2020b software. The wave force–motion module, depicted in Figure 16, overlays the force of the T-foil with the mathematical model of the ship, the encountered wave's parameters (wavelength, wave height, etc.), and the ship model's speed as inputs to determine the total force of the ship subjected to the disturbing force under each operating condition. The motion parameters of the ship model are derived using the transfer function $G(s)$, as seen in Figure 17. The four elements of the $G(s)$ matrix (Equation (12)) are represented by G11, G12, G21, and G22. The swing angle calculation module receives the output of these calculations, as illustrated in Figure 18. The swing angle φ of the T-foil is obtained by the given control parameter C_{ij}, where $C_1' = 1 - \frac{C_1}{K_F l_F}$, $C_2' = \frac{l_F}{U} - \frac{C_2}{K_F l_F}$, $C_3' = -\frac{C_3}{K_F l_F}$. The module responsible for calculating the lift force (moment) is depicted in Figure 19. Based on the value of the determined control parameter, Equation (2) yields the real-time lift force (moment) produced by the T-foil, which is then fed back to the wave force–motion module to prevent the hull from moving longitudinally.

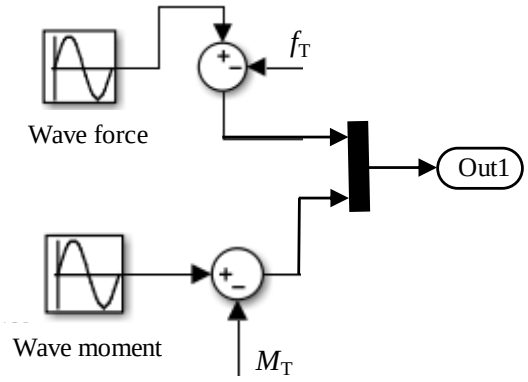

Figure 16. Wave-force module.

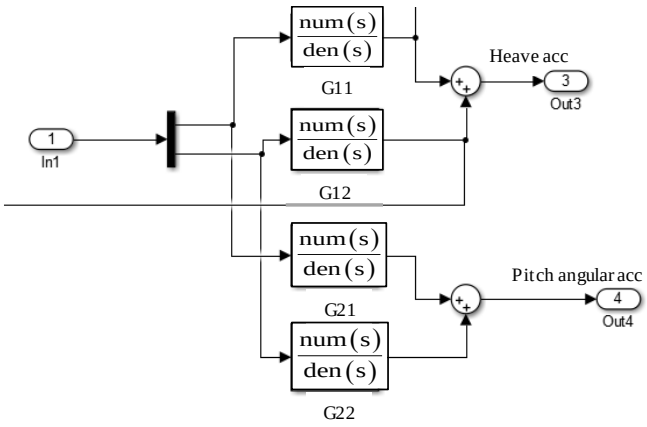

Figure 17. Force–motion module.

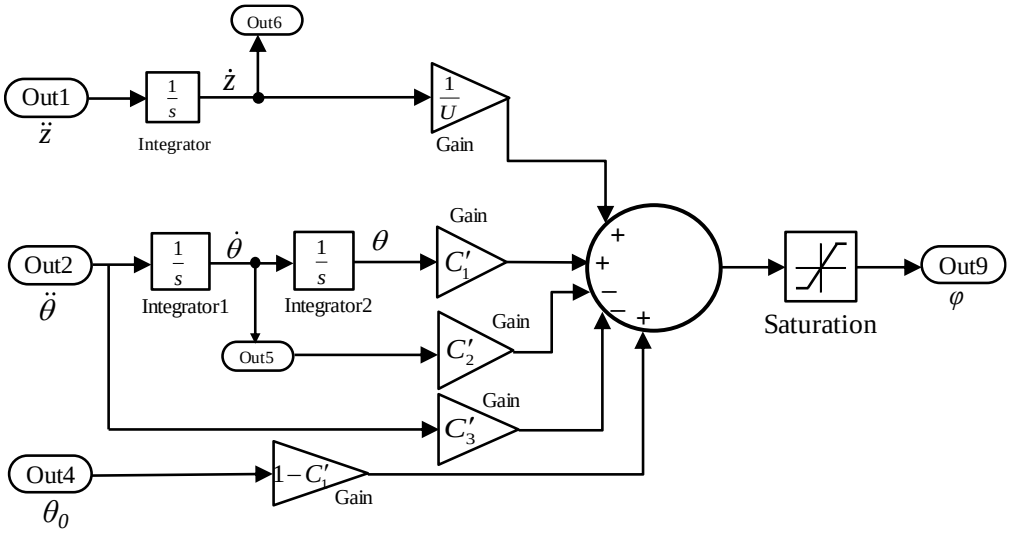

Figure 18. Swinging angle control module.

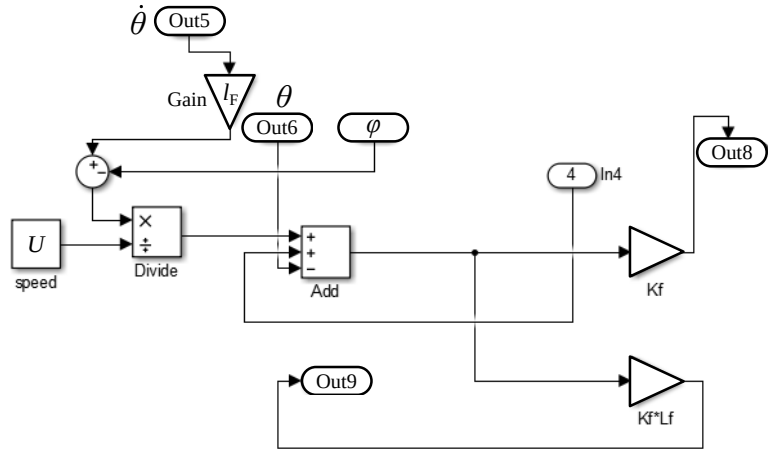

Figure 19. Lift force calculation module.

4.3. Calculation of Hydrodynamic Coefficients

To determine the hydrodynamic coefficients of a single mode with a specified amplitude and frequency, the model is forced to oscillate using the CFD technique in a viscous numerical pool. With the pure heave motion as an example, the motion amplitude of the forced heave is x_{30}, so the pure heave motion can be expressed as

$$x_3 = x_{30} \sin \omega t \tag{13}$$

The force F_{33} and moment M_{53} of the ship can be obtained from STAR CCM+, and the force equation is

$$\begin{cases} A_{33}\ddot{x}_3 + B_{33}\dot{x}_3 + F_{33} = 0 \\ A_{53}\ddot{x}_3 + B_{53}\dot{x}_3 + M_{53} = 0 \end{cases} \tag{14}$$

The vertical forces (moments) were fitted according to the least squares method:

$$\begin{cases} F_{33} = F_{3A} \sin \omega t + F_{3B} \cos \omega t \\ M_{53} = M_{5A} \sin \omega t + M_{5B} \cos \omega t \end{cases} \tag{15}$$

where F_{3A}, F_{3B}, M_{5A}, and M_{5B} are the amplitudes after least-squares fitting, and the additional mass coefficients and damping coefficients can be obtained by association:

$$A_{33} = \frac{F_{3A}}{x_{30}\omega^2},\ A_{53} = \frac{M_{5A}}{x_{30}\omega^2},\ B_{33} = -\frac{F_{3B}}{x_{30}\omega},\ B_{53} = -\frac{M_{5B}}{x_{30}\omega} \tag{16}$$

The same method is used to obtain the six degrees of freedom and their coupled additional mass and damping. The equations of each unfactorized hydrodynamic coefficient and wave force (moment) in this computation are displayed in Equation (17), where every parameter is satisfied:

$$\begin{array}{l}\omega' = \omega\sqrt{L/g},\ A'_{33} = A_{33}/\rho\nabla,\ A'_{55} = A_{55}/\rho\nabla L^2, B'_{33} = B_{33}/\rho\nabla\sqrt{g/L},\\ B'_{55} = B_{55}/\rho\nabla L^2\sqrt{g/L},\ A'_{53} = A_{53}/\rho\nabla L,\ B'_{53} = B_{53}/\rho\nabla L\sqrt{g/L},\\ A'_{35} = A_{35}/\rho\nabla L,\ B'_{35} = B_{35}/\rho\nabla L\sqrt{g/L}, F'_3 = 2F_3/(H\cdot C_{33}), M'_5 = 2M_5/(kH\cdot C_{55})\end{array} \tag{17}$$

4.4. Simlation Results

The simulation of active control is conducted at two speeds, U = 2.115 m/s and 3.2 m/s, and wavelength $\lambda \in [3, 10]$. The ship's pitch angle and heave amplitude are computed for each encounter frequency. Three types of T-foils are included in the calculation objects: T-foil without control, T-foil controlled by pitch angle signal, and T-foil controlled by optimized phase lag. STAR CCM+ is used to calculate the motion response of the fixed T-foil, while Simulink simulation is used to compute the motion response of the actively controlled T-foil. The method of using a pitch angle signal to control the T-foil is referenced [21], and its control equation is simplified from Equation (6) as

$$\varphi = (1 - \frac{C_1}{K_F l_F})\theta - \frac{l_F}{U}\dot{\theta} + \frac{1}{U}\dot{z} + \frac{C_1}{K_F l_F}\theta_0 \tag{18}$$

The method of determining the control parameter C_1 is as described above.

4.4.1. Time-Record Curves

Figure 20 presents the time-record curves (λ = 6 m) of T-foil angle φ, heave z, and pitch angle θ. Under phase lag control, the swing angle phase precedes the pitch angle control phase by about 0.3 s. The swing angle also leads both pitch and heave motion. Due to the phase difference between pitch motion and wave exciting force, phase lag control advances the lift force (and moment) phase. This reduces negative feedback stemming from phase issues, enhancing anti-vertical motion effectiveness. The effect is limited at low speeds due to the lift force being significantly smaller than the wave exciting force. However, as speed increases, heave and pitch motions are reduced by over 25% compared to pitch angle control.

4.4.2. Frequency Response Curves

The frequency response curves of heave and pitch at different speeds are shown in Figures 21–24. The response amplitude of the ship's heave at a low speed varies with the encounter frequency (ω_e) under different operational conditions (Figure 21). The amplitude of the heaves is the ordinate. The ship's motion peaks at wavelengths of 4 and 10 m while a fixed T-foil is in service. The T-foil can be more noticeable in operating conditions when the wavelength of the regular wave is close to the length of the ship. When the wavelength of the regular wave is in conditions of $\lambda/L < 1$ and $\lambda/L > 2$, the ship's response under the pitch angle control signal is slightly higher than that without turning. The ship's heave response can be further reduced in most working conditions, particularly in short-wave working conditions, after phase lag optimization. Additionally, the anti-vertical motion effect increases by more than 20% when compared to the static T-foil and by more than 10% when compared to the pre-optimization. This is because the phase lag problem is more obvious in the case of a short wave than in the case of a long wave, and an appropriately advanced lift (moment) phase can further improve the effect.

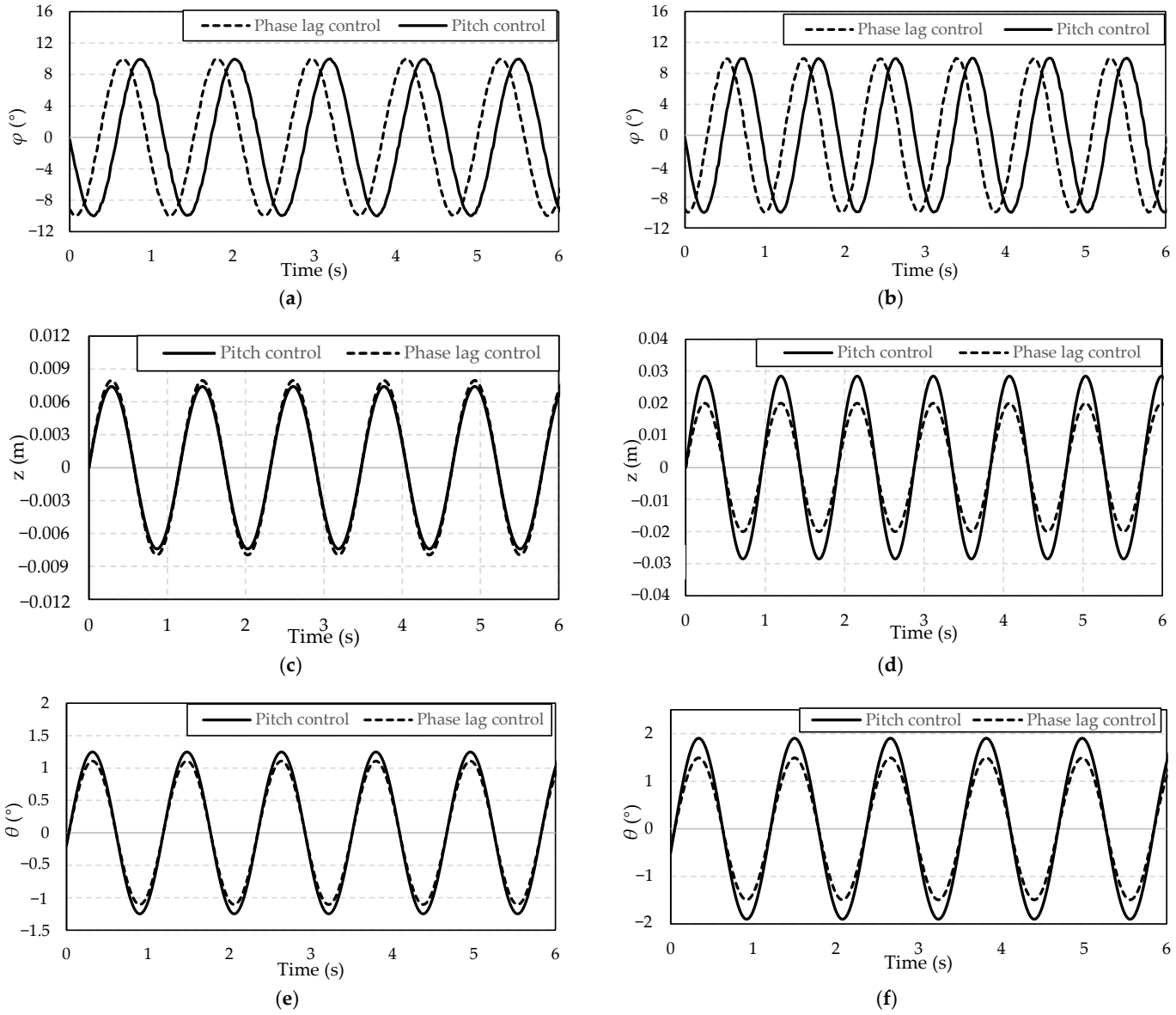

Figure 20. Time-record curves of different speeds (λ = 6 m). (**a**) Time-record curves of swing angle φ (*Fr* = 0.3). (**b**) Time-record curves of swing angle φ (*Fr* = 0.5). (**c**) Time-record curves of heave (*Fr* = 0.3). (**d**) Time-record curves of heave (*Fr* = 0.5). (**e**) Time-record curves of pitch (*Fr* = 0.3). (**f**) Time-record curves of pitch (*Fr* = 0.5).

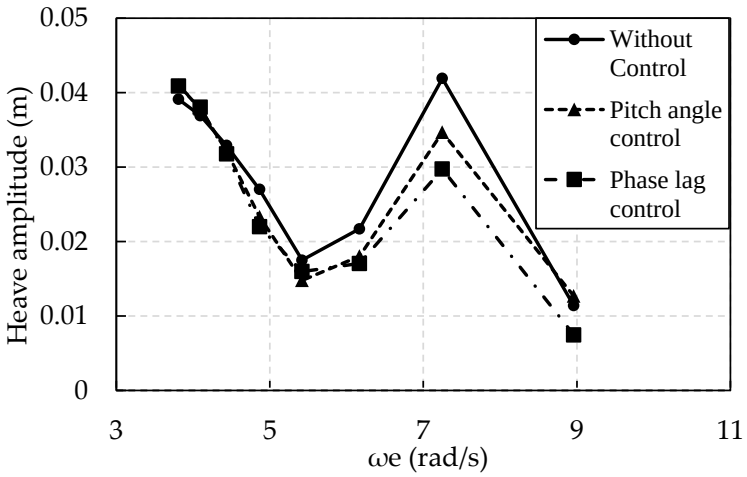

Figure 21. Heave amplitude in different control methods (*Fr* = 0.3).

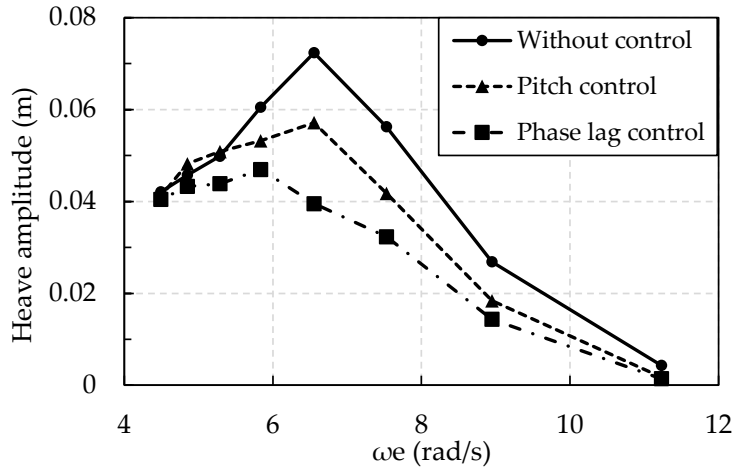

Figure 22. Heave amplitude in different control methods (*Fr* = 0.5).

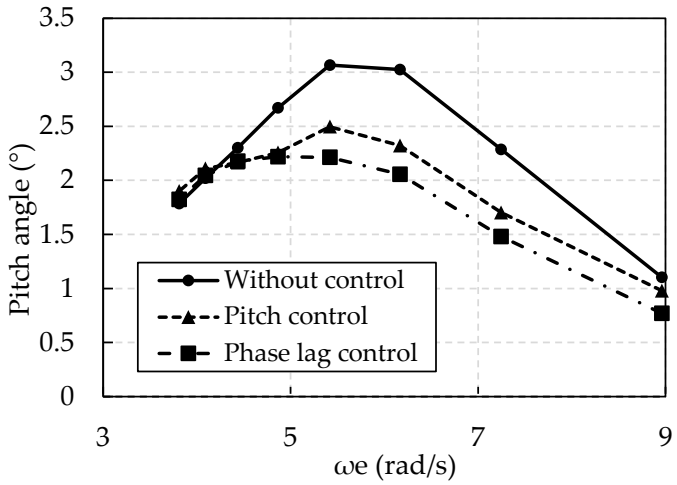

Figure 23. Pitch amplitude in different control methods (*Fr* = 0.3).

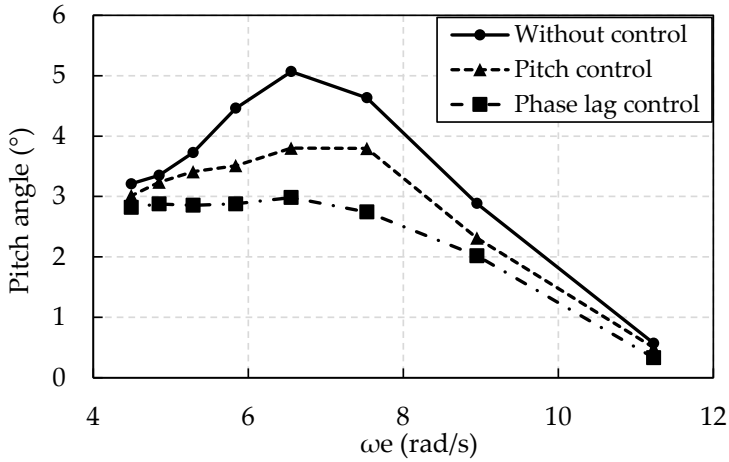

Figure 24. Pitch amplitude in different control methods (Fr = 0.5).

The ship's heave amplitude is much greater at high speeds than it is at low ones, and the response's variation trend in each frequency band differs noticeably from that of low speeds as well. As shown in Figure 22, the peak of the ship's motion is located at λ = 6 m and ω_e = 6.55 rad/s. The low response value of the T-foil makes its effect less noticeable in short-wave operating conditions. Within the high response area ($1 \leq \lambda/L < 2$), the active T-foil may effectively counteract vertical motion using two control methods, and pitch angle adjustment can effectively suppress vertical motion by more than 20%. This is due to the lift force's direction, which limits movement, being opposite to the pitch's direction and its phase's direction being contrary to the heave's direction. When accounting for phase latency, the effect can be enhanced by an additional 20% and decreased by 45% when compared to a static T-foil. The effect of the two control methods is minimal because, similar to the low speed, the wave force is bigger in the long band, but the T-foil's lift force is limited, and the phase lag effect is smaller.

For pitch motion, the variation of pitch angle with encounter frequency under various working conditions is shown in Figures 23 and 24. At low speed, under the action of a fixed T-foil, the pitch angle of the ship can reach 3°, and the response value is higher under the condition of the wavelength being similar to the length of the ship ($1 \leq \lambda/L \leq 1.5$). When the pitch angle signal is utilized, the active T-foil may reduce the pitch angle by more than 0.5°, and the anti-vertical motion percentage is almost 20%. The impact is further enhanced by roughly 10% upon the addition of optimized phase lag. When the pitch angle signal is utilized to regulate the lift force (moment) of the T-foil, its effect on the pitch is more evident due to the modest difference in phase between heave and pitch motion. The peak value of pitch motion is greatly diminished, particularly when taking phase lag management into account. Nevertheless, the motion response in the condition of long wavelength ($\lambda/L \geq 2$) under this control method is significantly higher than that under other conditions, which lessens the influence of the encountering wave's length on the pitch motion because the T-foil finds it difficult to play an obvious anti-vertical motion role in the long band.

When traveling at a high speed, as demonstrated in Figure 24, the fixed-foil action is applied when the pitch motion peak exceeds 5° at λ/L = 1.5. When compared to low speed, the T-foil's influence is more noticeable. In high-response situations, the pitch angle can be lowered by almost 2°, and the actively controlled T-foil performs well under all operating circumstances. After the addition of optimized phase lag, the pitch angle can be reduced by more than 40% compared with the static T-foil's control, and it can also be reduced by more than 10% for a long band. This is because the pitch angle restriction is more noticeable and the T-foil's lift force is much higher at high speeds than it is at low speeds. Pitch response must be reduced by around 20% at high speeds, and this can be achieved using the optimized control method in comparison to the pitch angle's control method without taking phase lag into account.

The difference in the anti-vertical motion effect between the two control methods is minimal for long wave conditions ($\lambda/L \geq 2$, Figures 21–24). This is attributed to the higher wave exciting force at longer wavelengths, rendering the T-foil's lift force less impactful. In addition, the phase difference between wave force and motion is small for $\lambda/L \geq 2$ due to the long encounter period, leading to similar results for both control methods. In the high response region ($1 < \lambda/L < 2$), the lift force phase in phase lag control precedes motion, with minimal deviation from the wave force phase, resulting in better suppression of wave influence. At $\lambda/L \leq 1$, motion amplitude is low, limiting the T-foil's effect.

5. Conclusions

In this article, we have developed a control system to limit the vertical motion of a trimaran via a T-foil. After the static lift value of the T-foil under various angles of attack was calculated using CFD technology, the lift force of the T-foil under dynamic control was approximated through the linear fitting, completing the lift modeling of the T-foil. Based on this, the phase difference between lift force and motion in still water was discussed. Following this, the T-foil's control equation was optimized, taking into account the phase lag effect. The swing angle of the T-foil was then controlled by the pitch angle, pitch angular velocity, and pitch angular acceleration. Finally, the motion response of the ship in regular waves was calculated through dynamic simulation. The impacts of the two control strategies were then compared, and the following conclusions were drawn:

(1) When sailing in still water, the lift force (moment) generated during the swing of the T-foil produces a relatively obvious vertical motion on the ship. Although the phase lags slightly, the frequency of the ship's motion caused by the T-foil's periodic lift force (moment) oscillates at a frequency that is compatible with the oscillation frequency of the T-foil. The lag time of heave and pitch motion is approximately 0.3 times the swing period, and the phase of heave and pitch motion is close when the lift force swing frequency is large. At lower frequencies, when the lift of the T-foil operates on the ship, the phase lag issue is less noticeable than that at higher frequencies. The phase lag issue is unavoidable given that the ship exhibits a significant motion reaction in regular waves with high encounter frequencies.

(2) The introduction of an active control method in trimaran sailing in regular waves can effectively reduce the ship's heave and pitch motion. Especially in the high response area, compared with the static T-foil, the suppression effect on pitch and heave is increased by more than 40%, and the effect is more obvious at a high speed. In comparison to the previously employed pitch motion control, the phase hysteresis control has a superior effect and can improve the effect by 20%. This is because the encounter frequency corresponding to the high response area is also higher, making the hysteresis effect of lift force more visible at this time. In the long band, due to the high wave force and the weak lift lag effect, the anti-vertical motion effect of the T-foil is not obvious under the two active control methods.

(3) The static airfoil theory was used to calculate the lift force in this work. However, the lift force generated by the rotation of the T-foil is a component of the dynamic lift force, so if the dynamic lift force is calculated and fitted, it will be more practical. Additionally, the multi-signal control parameter calculation method used in this study is only relevant to regular waves, and it needs to be further optimized for application to real-world sailing conditions.

Author Contributions: Conceptualization, Y.S.; methodology, Y.S. and G.J.; software, D.Z.; formal analysis, Y.S. and Y.W.; data curation, Z.W.; writing—original draft preparation, Y.S.; writing—review and editing, D.Z.; supervision, D.Z.; funding acquisition, Y.S. and D.Z. All authors have read and agreed to the published version of the manuscript.

Funding: This research was funded by the Program for Scientific Research Start-up Funds of Guangdong Ocean University, grant number 060302072102, and Zhanjiang Marine Youth Talent Project-Comparative Study, grant number 2021E5007.

Institutional Review Board Statement: The study did not require ethical approval.

Informed Consent Statement: The study did not involve humans.

Data Availability Statement: The data that support the findings of this study are available from the corresponding author, upon reasonable request.

Conflicts of Interest: The authors declare no conflicts of interest.

References

1. Davis, M.R.; Holloway, D.S. A comparison of the motions of trimaran, catamarans and monohulls. *Aust. J. Mech. Eng.* **2007**, *4*, 183–195. [CrossRef]
2. Zhang, S.T.; Sun, M.X.; Liang, L.H.; Jiang, J.L. A controller design using state-feedback H∞ method for T-foil of passive control. *Ship Sci. Technol.* **2014**, *36*, 78–82.
3. Lau, C.Y.; Ali-Lavroff, J.; Holloway, D.S.; Alavimehr, J.A.; Thomas, G.A. Influence of an active T-foil on motions and passenger comfort of a large high-speed wave-piercing catamaran based on sea trials. *J. Mar. Sci. Technol.* **2022**, *27*, 856–872. [CrossRef]
4. Hebblewhite, K.; Sahoo, P.K.; Doctors, L.J. A case study: Theoretical and experimental analysis of motion characteristics of a trimaran hull form. *Ships Offshore Struct.* **2007**, *2*, 149–156. [CrossRef]
5. Li, P.Y.; Qiu, Y.M.; Gu, M.T. Study of trimaran wavemaking resistance with numerical calculation and experiments. *J. Hydrodyn.* **2002**, *14*, 99–105.
6. Xu, M.; Zhang, S.L.; Klakak, P. A numerical study on side hull optimization for trimaran. *J. Hydrodyn. Ser. B* **2011**, *23*, 695–702. [CrossRef]
7. Haywood, A.J.; Duncan, A.J.; Klakak, P.; Bennett, J. The development of a ride control system for fast ferries. *Control. Eng. Pract.* **1995**, *3*, 695–702. [CrossRef]
8. Fang, M.C.; Shyu, W.J. Improved prediction of hydrodynamic characters of SWATH ships in wave. *Proc. Natl. Sci. Counc.* **1994**, *18*, 495–507.
9. Davis, M.R.; Watson, N.L.; Holloway, D.S. Wave response of an 86 m high speed catamaran with active T-foils and stern tabs. *Trans. R. Inst. Nav. Archit. Part A Int. J. Marit. Eng.* **2003**, *145*, 15–34.
10. De LA Cruze, J.; Aranda, J.; Giron-Sierra, J.M.; Velasco, F.; Andres-Toro, B.D. Improving the comfort of a fast ferry. *IEEE Control. Syst.* **2004**, *24*, 47–60.
11. Esteban, S.; Giron-Sierra, J.M.; De Andres-Toro, B.; Cruz, J.D.; Riola, J.M. Fast ships models for seakeeping improvement studies using flaps and T-foil. *Math. Comput. Model.* **2005**, *41*, 1–24. [CrossRef]
12. Giron-Sierra, J.M.; Esteban, S.; Cruz, J.M.; Andres, B.D.; De LA Cruze, J.; Riola, J.M. Fast ship's longitudinal motion attenuation with T-Foil and flaps. In Proceedings of the Novel Vehicle Concepts and Emerging Vehicle Technologies Symposium, Ottawa, ON, Canada, 18–21 October 1999; The RTO Applied Vehicle Technology Panel: Neuilly-sur-Seine, France, 2003; pp. 26–34.
13. Esteban, S.; Giron-Sierra, J.M.; Andres, B.D.; Cruz, J.M. Development of a control-oriented model of the vertical motions of a fast ferry. *J. Ship Res.* **2004**, *48*, 218–230. [CrossRef]
14. Alavimehr, J. The Influence of Ride Control System on the Motion and Load Response of a Hydroelastic Segmented Catamaran Model. Ph.D. Thesis, University of Tasmania, Hobart, Australia, 2016.
15. Javad, A.M.; Jason, L.; Davis, M.R.; Damien, S.; Holloway, G.A. An experimental investigation of ride control algorithms for high-speed catamarans Part 1: Reduction of ship motions. *J. Ship Res.* **2017**, *61*, 35–49.
16. Jiang, Y.C.; Bai, J.Y.; Sun, Y.; Sun, Y.F.; Zong, Z. Numerical investigation of T-Foil hybrid control strategy for ship motion reduction in head seas. *Ocean Eng.* **2020**, *217*, 107924. [CrossRef]
17. Jiang, Y.C.; Bai, J.Y.; Liu, S.J.; Zong, Z.; Li, P. Experimental investigation of T-foil hybrid control strategy for ship motion reduction in head seas. *Ocean Eng.* **2022**, *243*, 110251. [CrossRef]
18. Liu, Z.L.; Zheng, L.H.; Li, G.S.; Yuan, S.Z.; Yang, S.B. An experimental study of the vertical stabilization control of a trimaran using an actively controlled T-foil and flap. *Ocean Eng.* **2021**, *219*, 108224. [CrossRef]
19. López, R.; Santos, M. Neuro-Fuzzy system to control the fast ferry vertical acceleration. In Proceedings of the 15th IFAC World Congress, Barcelona, Spain, 21–26 July 2002; pp. 319–324.
20. Jia, J.B.; Zong, Z.; Shi, H.Q. Model experiments of a trimaran with transom stern. *Int. Shipbuild. Prog.* **2009**, *56*, 119–133.
21. Zong, Z.; Sun, Y.F.; Jiang, Y.C. Experimental study of controlled T-foil for vertical acceleration reduction of a trimaran. *J. Mar. Sci. Technol.* **2019**, *24*, 553–564. [CrossRef]